Performance-Based Optimization Considering Both Structural and Nonstructural Components

Hugo A. Rojas,[a] M.EERI, Shahram Pezeshk,[b] M.EERI, and Christopher M. Foley,[c] M.EERI

Development of performance-based design (PBD) methodologies for buildings and a better understanding of the performance and damage to nonstructural components during ground motion events give rise to design problems that involve structural and nonstructural component performance. The current research effort is geared toward development of an automated PBD environment to optimize structural system performance. FEMA-350 and HAZUS procedures are used to evaluate confidence levels associated with the probability of a structure not meeting targeted performance levels. A genetic algorithm (GA) is used to solve this complex optimization problem where confidence levels are incorporated into a GA fitness function along with initial construction cost in a series of optimal design scenarios. Inelastic time-history analysis is used to evaluate the designs under different levels of hazard during execution of the evolutionary algorithm. Different optimization formulations are studied in order to explore the symbiotic relationship between seismic hazard magnitude, initial construction cost, and confidence levels for damage exceedance for structural and nonstructural components.
[DOI: 10.1193/1.2754002]

INTRODUCTION

There are significant sources of uncertainty with design for natural events (wind and earthquake), which give rise to complex design problems that involve structural and nonstructural component performance, and the risk of exceeding damage states. Next-generation structural design methodologies are intended to mitigate expected loss resulting from these hazards and performance-based engineering is destined to become the basis for next-generation structural design.

The development of performance-based design specifications and model codes for steel and concrete building structural systems (ATC 1996, FEMA 2000) has ushered in new applications of evolutionary computation in optimized structural design (Alimoradi 2004, Liu 2004). Performance-based structural optimization (PBSO) formulations often involve multiple-objective optimization problem statements. The constraints often in-

[a] Graduate Research Assistant, The University of Memphis, TN 38152; E-mail: harojas@memphis.edu
[b] Emison Professor, The University of Memphis, TN 38152; E-mail: spezeshk@memphis.edu
[c] Associate Professor, Marquette University, Milwaukee, WI 53201; E-mail: chris.foley@marquette.edu

Earthquake Spectra, Volume 23, No. 3, pages 685–709, August 2007;

volve target probabilities and/or confidence levels in meeting performance objectives. Efforts that involve minimum life-cycle cost design also fall into this category of structural optimization efforts.

Life-cycle cost optimization for steel framing systems has been a very fertile area of research that can be classified as PBSO. When the structural system life-cycle is included in the optimization, various ground motion levels need to be considered. U.S. design specifications and nonlinear pushover analysis have been used in conjunction with a genetic algorithm to solve a performance-based structural optimization problem that involved objectives related to initial construction expense (material weight), the number of different steel sections used in the design (diversity), and future seismic risk associated with interstory drift resulting from both frequent and infrequent ground motions (Liu et al. 2005). Lifetime seismic damage and initial material cost have also been considered as objectives in a GA-based optimization algorithm using nonlinear pushover analysis as the analytical basis for determining performance (Liu et al. 2003). Nonlinear pushover analysis used as the fitness-evaluation engine for genetic algorithms (Liu et al. 2004) and evolution strategies (Fragiadakis et al. 2006) has been used to solve PBSO problems involving objectives of minimum structure weight and confidence levels in meeting performance objectives during frequent and infrequent ground motion events.

While static pushover analysis is a useful method for defining performance expectations during ground motion events, it is well known that this analytical method tends to give inaccurate results for irregular structural systems. Inelastic time-history analysis (THA) is a better predictor of performance during ground motion events when compared to pushover analysis methodologies assuming ground motion characteristics, site characteristics, and structural system characteristics are reasonably quantified. Inelastic THA has been implemented as the foundation of multiple-objective PBSO for 2-D frame structures using genetic algorithms (Alimoradi 2004, Alimoradi et al. 2004, Alimoradi et al. 2007, Foley et al. 2007). In order to consider multiple objectives in the GA, a novel radial fitness was defined (Alimoradi 2004, Foley et al. 2007). The objective in these efforts for the PBSO statement was confidence in meeting performance objectives during frequent and infrequent ground motion events.

Historical applications of performance-based optimal design have ignored nonstructural components in the evaluation of performance. Although the process toward understanding nonstructural component performance was begun some time ago (Algan 1982), significant improvements in understanding nonstructural component performance have been made only recently (Comerio et al. 2002, Filiatrault et al. 2002, FEMA 2003, Holmes and Comerio 2003, Taghavi and Miranda 2003).

A risk-based structural design problem can be stated as: (1) minimize the initial cost of construction for the structural system; (2) ensure a tolerable level of risk against collapse for ground motions with less than 2% probability of exceedance in 50 years; and (3) ensure a tolerable level of risk of not being able to immediately occupy a building structure after an event with less than 50% probability of exceedance in 50 years. Recent developments make automating design problems such as these feasible. Alimoradi (2004) and Alimoradi et al. (2004) were among of the first researchers to consider the

performance-based earthquake engineering (PBEE) methodology within the automated and optimal design environment, and have laid the groundwork for algorithm development in this regard. Foley (2002) laid out a schematic methodology for PBE optimization within the realm of gravity load, wind load, and seismic loading. The objective of the present research effort is to explore the symbiotic relationship between seismic hazard magnitude, initial construction cost, and confidence levels for damage exceedance for structural and nonstructural components using inelastic THA- and GA-based optimization methodologies to automate structural design.

The process used to achieve the objective begins with generation of acceleration time histories for multilevel ground motion events. FEMA-350 procedures (FEMA 2000) are used to define and assess structural component damage, and HAZUS methodologies (FEMA 2003) are used to define and assess nonstructural component damage. These two methodologies are synthesized to facilitate computation of confidence levels against damage exceedance for structural and nonstructural components. A risk-based design optimization problem with appropriate loading conditions and constraints is formulated. The design problem is solved using an evolutionary computation that has seen a considerable number of applications in the field of structural and earthquake engineering (Pezeshk et al. 1997, Kim and Ghaboussi 1999, Pezeshk et al. 2000, Schinler and Foley 2001, Alimoradi and Ahmadi 2002, Foley et al. 2002, Foley and Schinler 2003, Alimoradi 2004, Naeim et al. 2004, Liu et al. 2006).

PROBABILISTIC PERFORMANCE-BASED DESIGN

Buildings are composed of both structural and nonstructural systems. While damage to the structural system is the most important measure of building damage affecting casualties and catastrophic loss of life, damage to nonstructural systems and contents can result in significant economic and human loss through building-facility downtime, content damage, and injury or death. Typically, the structural system represents about 25% of the building's worth (FEMA 2003). Relatively recent urban earthquakes proved that it is very important to consider nonstructural damage in the design phase rather than exclusively targeting structural performance. Therefore, the formulation used in this paper attempts to predict separately the performance of: (1) the structural system; (2) nonstructural drift-sensitive (NSD) components, such as partition walls, that are primarily affected by building interstory displacement; and (3) nonstructural acceleration-sensitive (NSA) components, such as suspended ceilings, that are primarily affected by building shaking. FEMA-350 (FEMA 2000) and HAZUS (FEMA 2003) procedures allow both structural and nonstructural damage to include confidence levels for attaining expected performance.

STRUCTURAL COMPONENTS

The FEMA-350 (FEMA 2000) procedure is defined as demand and resistant factor design (DRFD). The basic premise of the DRFD procedure is to establish a confidence parameter,

Table 1. Confidence evaluation parameters for special moment frames (SAC 2000)

IO Performance	CP Performance
β_{UT}=0.20	β_{UT}=0.30
C=0.02	C=0.10
ϕ=1.0	ϕ=0.9
γ=1.5	γ=1.3
γ_a=1.02	γ_a=1.03

$$\lambda = \frac{\gamma \cdot \gamma_a \cdot D}{\phi \cdot C} \tag{1}$$

where D is the calculated median-value demand obtained via structural analysis, C is the median capacity estimate for the corresponding demand quantity, γ is the demand variability factor, γ_a is the analysis uncertainty factor, and ϕ is the capacity reduction factor. A thorough discussion of the technical framework for DRFD is available (Jalayer and Cornell 2003).

Global interstory drift is presently used as a measure of structural demand and capacity for evaluating Equation 1 at each performance level. A confidence parameter obtained for a given design is used to back-calculate the design's confidence level as follows:

$$\lambda = e^{-b\beta_{UT}(K_x - k\beta_{UT}/2)} \tag{2}$$

where b is a coefficient relating the incremental change in demand to an incremental change in ground motion intensity (b=1.0 implies linear relationship); β_{UT} is an uncertainty measure equal to the vector sum of the logarithmic standard deviation of the variations of demand and capacity; k is the slope of the hazard curve in natural logarithm coordinates at the hazard level of interest (its magnitude is taken to be 3.00 for this present study); and K_x is the standard Gaussian variate associated with the probability of x not being exceeded as a function of number of standard deviations above or below the mean, from standard probability tables.

Table 1 contains the uncertainty coefficients, capacities, capacity reduction factors, analysis uncertainty, and demand variability factors considered for each performance level used in the present analyses. If λ is calculated using Equation 1 for a given series of ground motion records corresponding to a performance objective, the standard normal variable, K_x, can be computed using Equation 2 and a corresponding confidence

level for that performance being met can be computed using

$$q = \Phi(K_x) = \frac{1}{2}\, erfc\left\{ \frac{-K_x}{\sqrt{2}} \right\} \tag{3}$$

where $erfc\{\ \}$ is the complementary error function; and $\Phi(K_x)$ denotes the normal cumulative distribution function value corresponding to K_x.

FEMA 350 (FEMA 2000) presents procedures for two discrete structural performance levels: immediate occupancy (IO) and collapse prevention (CP). IO-level design is responsible for controlling the functionality of facilities and economic loss after an earthquake, while CP-level design mainly controls the loss of life and number of casualties. For the present study, the confidence of a design meeting the CP performance objective is met though evaluating confidence parameters for a suite of seven ground motions with 2% probability of exceedance in a 50-year exposure period. Confidence in meeting IO performance is evaluated using a suite of seven ground motion–acceleration time histories with 50% probability of exceedance in a 50-year exposure period.

NONSTRUCTURAL COMPONENTS

The HAZUS earthquake loss-estimation methodology is a complex collection of components that work together to estimate casualties, loss of function, and economic impacts on a region due to a scenario earthquake. Despite its reliance on expert opinion rather than experimental results for its fragility functions, HAZUS is widely known and still represents something of a U.S. and international standard. One of the main components of the methodology is estimating the probability of various states of structural and nonstructural damage to buildings (FEMA 2003). The structural-engineering community has recently conducted research seeking to define fragility functions for specific nonstructural components similar to those used by the HAZUS methodology (Taghavi and Miranda 2003). The completeness of the HAZUS methodology makes it attractive for the present research effort even though one may consider its fragility curve formulations to be not as complete as the newly proposed methods.

HAZUS damage functions for ground shaking have two basic components: (1) capacity curves and (2) fragility curves. The capacity curves are based on engineering parameters that characterize the nonlinear behavior of a building type. The fragility curves describe the probability of damage to the building's: (1) structural system, (2) NSD components, and (3) NSA components.

Building fragility curves are lognormal functions that describe the probability of reaching, or exceeding, structural and nonstructural damage states, given median estimates of spectral response quantities such as spectral displacement (FEMA 2003). In this study, damage to nonstructural components is described by five discrete damage states: none, slight, moderate, extensive, or complete. Therefore, for a given level of building response, fragility curves distribute damage among these five physical damage states. Each fragility curve is defined by a median value of the demand parameter (e.g., spectral displacement) that corresponds to the exceedance threshold and variability associated with a damage state (FEMA 2003).

Table 2. Fragility curve parameters for nonstructural components for S1L building type and high-code seismic design level (FEMA 2003)

Nonstructural Component	Curve Parameter	Damage State			
		Slight	Moderate	Extensive	Complete
NSD	$\overline{ISDA_{ds}}$	0.004	0.008	0.025	0.050
	β_{ds}	0.50	0.50	0.50	0.50
NSA	$\overline{PFA_{ds}}$ (g)	0.30	0.60	1.20	2.40
	β_{ds}	0.60	0.60	0.60	0.60

The conditional probability of being in, or exceeding, a particular damage state, *ds*, given any engineering demand parameter, *EDP*, is computed using the normal cumulative distribution function, Φ, given by Equation 4:

$$P[ds|EDP] = \Phi\left[\frac{1}{\beta_{ds}} \cdot \ln \frac{EDP}{\overline{EDP_{ds}}}\right] \tag{4}$$

where $\overline{EDP_{ds}}$ is the median value of the *EDP* considered (e.g., interstory drift, floor acceleration) at which the threshold of a damage state, *ds*, is reached, and β_{ds} is the lognormal standard deviation of the *EDP* and *ds* considered.

Since Φ[ ] denotes the normal cumulative distribution function, the confidence level, q_{EDP}^{ds}, that a certain damage state or worse will not occur given an *EDP* can be computed using the complimentary probability

$$q_{EDP}^{ds} = 1 - P[ds|EDP]. \tag{5}$$

The interstory drift angle (ISDA) and the peak floor acceleration (PFA) are used to characterize the response of NSD and NSA components, respectively. The median values of these parameters ($\overline{ISDA_{ds}}$ and $\overline{PFA_{ds}}$) as well as the damage-state lognormal standard deviation, β_{ds}, for a high-code seismic design level (based on 1994 UBC lateral force design requirements of Seismic Zone 4) and a building type S1L (steel moment frames) according to FEMA 2003 are presented in Table 2.

OPTIMIZATION STATEMENT AND GA-BASED SOLUTION

In this research effort, a 50-year service life for the building is assumed. Two levels of ground motion are assumed to be important in characterizing structural and nonstructural damage and, therefore, building performance. The first is a relatively large event that is used to assess the CP performance objective. It is assumed to have a 2% probability of being exceeded in this 50-year window. The second is characterized by lower peak ground acceleration and is used to assess meeting the IO performance objective and to generate estimates for nonstructural damage. It has a much lower mean recurrence interval and it has a 50% probability of being exceeded in 50 years.

Using this two-level ground motion–magnitude approach, and maintaining the assumption of a 50-year service life for a building structure, a risk-based optimization problem can be described as follows:

1. Minimize the initial construction cost for the structural system, which is approximated by minimizing the total structural weight (W).
2. Seek a user-defined confidence level in meeting the CP performance objective for structural components.
3. Seek a user-defined confidence level in meeting the IO performance objective for structural components.
4. Seek user-defined confidence levels such that damages to NSD and/or NSA components will not be worse than those associated with a specified damage state (i.e., slight, moderate, extensive, and complete).
5. Adhere to strong-column weak-beam (SCWB) criteria of AISC (2005).

Minimizing the weight of a structural steel building system (such as that considered here) does not necessarily minimize the cost of the structural steel skeleton. Recent researchers (Liu et al. 2006) implemented fabrication complexity in their optimization formulation in recognition that fabrication cost is essential when evaluating economy of the structural steel system. Fabrication complexity in the form of penalty schemes has also been implemented (Foley et al. 2002, Foley and Schinler 2003). These other formulations intended to more accurately reflect that the initial construction cost can easily be incorporated into the present formulation.

Several constraints are considered in the optimization problem formulation. The first ensures a minimum user-defined confidence level for CP performance. FEMA-350 (FEMA 2000) recommends a minimum level of 90% for attaining CP performance. The second ensures a minimum confidence level for meeting IO performance. FEMA-350 (FEMA 2000) recommends a minimum level of 50% for confidence in attaining IO performance. HAZUS (FEMA 2003) is utilized to generate constraints that ensure user-defined levels of confidence in not exceeding damage states for nonstructural components. The constraints will be described in much greater detail in subsequent sections.

The fundamental probabilistic performance-based design optimization problem statement for frames considering structural and nonstructural damage is written as:

$$\min\{W\} \tag{6}$$

subject to:

$$q^{CP} = q^{CP}_{limit} = 0.95 \tag{7}$$

$$q^{IO} = q^{IO}_{limit} = \text{varies} \tag{8}$$

$$q^{ds}_{NSD} = q^{ds}_{NSD,limit} = \text{varies} \tag{9}$$

$$q^{ds}_{NSA} = q^{ds}_{NSA,limit} = \text{varies} \tag{10}$$

$$\left(\sum M_{p,col} \Big/ \sum M_{p,beam}\right)_{limit} = 1.20. \tag{11}$$

Performance has been included in the optimization statement through confidence levels. The confidence levels in meeting IO and CP performance for structural components are denoted as q^{CP} and q^{IO}, respectively. The confidence in meeting nonstructural performance at a desired damage state, *ds*, is defined as q^{ds}_{NSD} and q^{ds}_{NSA} for NSD and NSA components, respectively. Finally, q^{CP}_{limit}, q^{IO}_{limit}, $q^{ds}_{NSD,limit}$, and $q^{ds}_{NSA,limit}$ are the designer's limit on CP, IO, NSD, and NSA confidence levels, respectively.

This optimization problem is solved using a GA with the fitness of individual j at generation k during the evolution evaluated as:

$$F_{jk} = \alpha_w \left(\frac{W_{\max} - W_{jk}}{W_{\max}}\right) + \alpha_{CP} \cdot f^{CP}_{jk} + \alpha_{IO} \cdot f^{IO}_{jk} + \alpha_{NS} \cdot f^{NS,ds}_{jk} + \alpha_{SCWB} \cdot f^{SCWB}_{jk} \tag{12}$$

where the coefficients α_W, α_{CP}, α_{IO}, α_{NS}, and α_{SCWB} are the weights for each objective function, which should satisfy $\Sigma\alpha = 1$. Their values for the present study were set using a trial-and-error procedure and are presented in Table 4; $W_{\max}$ is the maximum possible weight for the topology; W_{jk} is the weight of design j in generation k; and f^{CP}_{jk}, f^{IO}_{jk}, $f^{NS,ds}_{jk}$, and f^{SCWB}_{jk} are fitness components for ensuring minimum user-defined confidence levels in meeting performance and for ensuring strong column-weak beam frame designs.

The fitness expressed in Equation 12 evolves from the inclusion of equality constraints in the optimization statement. The fitness is composed of one objective that is maximized and four objectives that are minimized. The maximized component of the fitness is the difference in the weight of an individual from the maximum weight that exists in the design space. The general form of the minimized components is given by:

$$f_j = \left(1 + \frac{|(p_{limit} - p_j)|}{p_{limit}}\right)^{\chi} \quad \text{where} \begin{cases} \chi = -3 & \text{if } p_j \leq p_{limit} \\ \chi = -1 & \text{if } p_j > p_{limit} \end{cases} \tag{13}$$

where p_{limit} is a user-defined limiting (or target) quantity, and p_j is the value of that quantity for individual j. The exponent, χ, helps to aid in convergence of solutions.

The values of p and the limits depend upon the constraint considered. If CP and IO performance-level constraints are considered, the values are:

$$p_{limit} = q^{CP}_{limit}, \quad p_j = q^{CP}_j \quad \text{and} \quad p_{limit} = q^{IO}_{limit}, \quad p_j = q^{IO}_j.$$

If nonstructural drift-sensitive and acceleration-sensitive constraints are considered, these values are:

$$p_{limit} = q^{ds}_{NSD,limit}, \quad p_j = q^{ds}_{NSD} \quad \text{and} \quad p_{limit} = q^{ds}_{NSA,limit}, \quad p_j = q^{ds}_{NSA}$$

where damage states, *ds*, are defined as slight, moderate, extensive, and complete (FEMA 2003). Therefore, the fitness components described by Equation 13 seek to minimize the difference between the user-defined target confidence levels and the confidence levels for any individual design.

The SCWB equality constraint is handled through the final component of the individual's fitness. The value of p_{limit} for this equality constraint is 1.2. The value of p for individual j now is the ratio for each beam-to-column joint i in the structural system:

$$p_j^i = \frac{\sum M_{p,col}}{\sum M_{p,beam}} \tag{14}$$

where $M_{p,col}$ and $M_{p,beam}$ are the plastic moment capacity of a column and a beam at joint i, respectively. The fitness for individual j at joint i is calculated using Equation 13; then the SCWB fitness component, used in Equation 12 to compute the total fitness for the individual j at generation k, is computed using:

$$f_{jk}^{SCWB} = \prod_{i=1}^{N_{jts}} f_j^i \tag{15}$$

where N_{jts} is the number of beam-to-column joints in the structure. This fitness component seeks to minimize the difference between the beam-to-column moment capacity ratios and 1.20.

It should be noted that the fitness components that address the equality constraints tend to penalize from both sides of the user-defined target. In other words, Equation 13 will establish a fitness component that is more favorable for those individuals where the value of p is close to the user-defined target. If the value is below the user-defined target, the fitness component is reduced more relative to a case where the value is above the user-defined target. The fitness component is maximized when the difference between p and the user-defined target is zero.

The computation of confidence levels, penalty functions, and fitness of an individual in the population is done using suites of ground motions and median values of maximum response quantities. The algorithm used to implement the GA in the solution to the optimization problem considered is given below.

1. Start with a randomly generated population of candidate solutions (possible designs) from the search space, which includes 256 AISC steel W sections.
2. For each individual (design) in a GA population, perform a nonlinear second-order THA of the structural model. Find the maximum response (e.g., peak interstory drift, peak floor accelerations) at each story level.
3. Repeat step 2 for each ground motion record in the 2/50 and 50/50 suites of ground motions considered.
4. Compute the median of the maximum response quantities (demands) for each set of ground motion records at each story level.
5. Find the maximum of median response demands over the whole structure and use it for confidence levels and fitness evaluations.

The confidence levels for IO and CP performances as well as the confidence level for any damage state for NSD components can be restated as interstory drift magnitudes using the FEMA-350 (FEMA 2000) and HAZUS (FEMA 2003) methodologies. Also,

Table 3. Interstory drift and floor acceleration limits corresponding to 50%, 75%, and 95% confidence

Ground Shaking Level	Performance Level		EDP Limit ($ISDA_{limit}$ or PFA_{limit} [g])		
			q_{limit}=50%	q_{limit}=75%	q_{limit}=95%
2/50	CP				0.04696
	IO		0.01388	0.01213	0.00999
	NSD	Slight	0.00400	0.00284	0.00175
		Moderate	0.00800	0.00572	0.00352
		Extensive	0.02500	0.01784	0.01099
50/50		Complete	0.05000	0.03569	0.02197
	NSA	Slight	0.30	0.20	0.11
		Moderate	0.60	0.40	0.22
		Extensive	1.20	0.80	0.44
		Complete	2.40	1.60	0.88

the confidence level for any damage state for NSA components can be restated as peak floor acceleration magnitudes using the HAZUS methodology (FEMA 2003). The drift and acceleration limits corresponding to 50%, 75%, and 95% confidence levels are shown in Table 3.

TWO-STORY FRAME EXAMPLE

The focus of the present effort will be on a planar structural steel moment-resisting frame with the topology shown in Figure 1. A special moment-resisting (SMR) frame will be considered. This frame is modeled using four design variables: one each for the columns and beam of the first floor, and one each for the columns and beam of the second floor. The structural steel used in the framework is A992 Grade 50-ksi. This material is used for all beams and columns. The lumped masses have a magnitude equal to $0.085 \cdot \mathrm{k} \cdot \mathrm{sec}^2/\mathrm{in}$.

The DRAIN-2DX computer program (Prakash et al. 1993) is used to carry out the inelastic THA required to evaluate the designs during execution of the evolutionary algorithm. DRAIN-2DX steel beam-column–type yield surface is used for columns and a beam-type surface (no P-M interaction) is used for the girder (Powell 1993). The yield surfaces for the beams and beam-columns in the frame used in the present study are shown in Figure 2. The axial tensile yield capacity of a beam-column in the absence of bending moment is defined as P_{yt}. This tensile force capacity is based upon the gross cross-sectional area and AISC (2005). The axial compression capacity of the beam column in the absence of bending moment is defined as P_{nc}^{minor} (AISC 2005). This axial load magnitude is the flexural-buckling capacity of the member about the minor axis of bending assuming that the unbraced length is the story height (150 inches) and the effective length factor is 1.0. M_p^+ and M_p^- are the positive and negative plastic moment capacities of the cross-section computed assuming no axial loading is present.

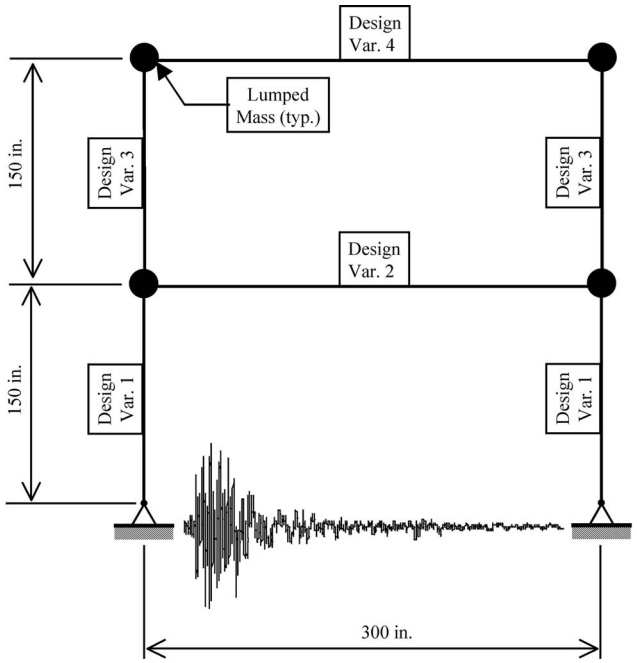

Figure 1. Two-story frame topology used in design example.

STRONG GROUND MOTION INPUT RECORDS

Seven pairs of strong ground motion records representing 2% and 50% probabilities of exceedance in 50 years for the city of Los Angeles were chosen from the records developed in the SAC steel project (Somerville et al. 1997). The selected records represent

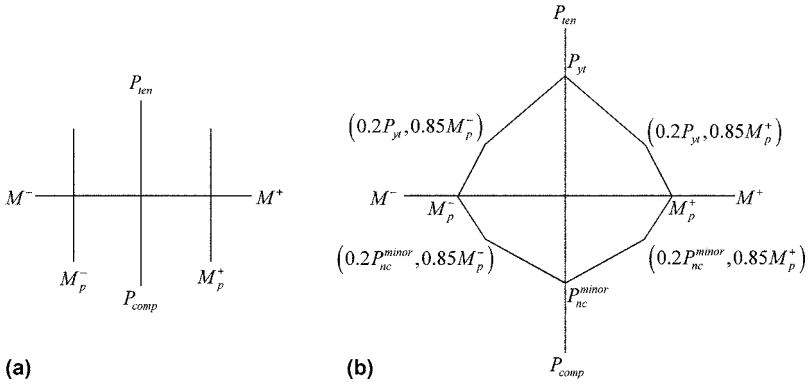

Figure 2. Yield surfaces assumed in the nonlinear response-history analysis: (a) beam member, and (b) beam-column member.

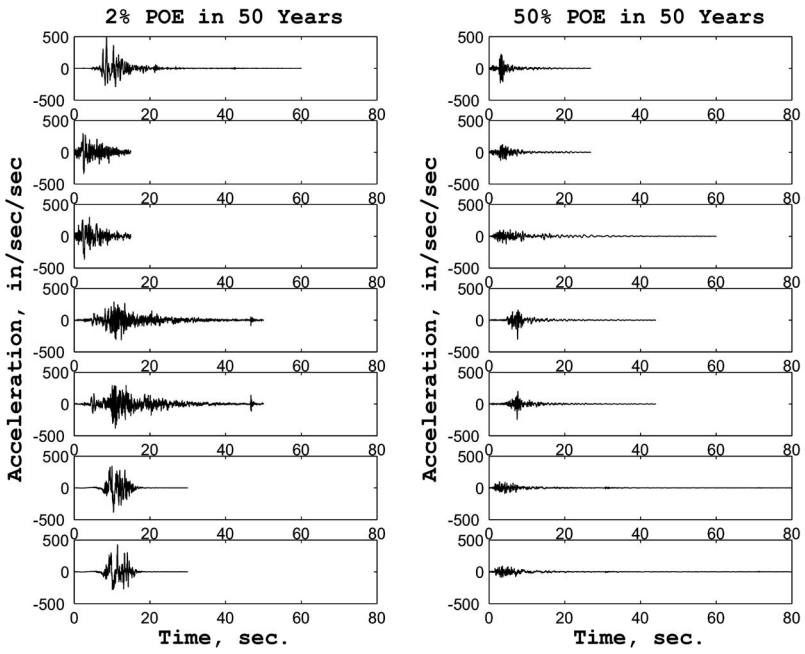

Figure 3. Input strong ground motion record sets used in the analyses (Somerville et al. 1997).

the target design spectra of NEHRP site category D (firm soil) with deaggregation of hazards of M6.75–7.5 at closest distance of 2–20 km, and M5–7 at 5–15 km for 2% and 50% probabilities of exceedance in 50 years, respectively (Somerville et al. 1997). These records, shown in Figure 3, are used as input for the analytical model to compute the median of maximum response quantities (i.e., interstory drift, floor acceleration) for the performance levels associated with the record probabilities.

GENETIC ALGORITHM PARAMETERS

An existing driver (Carroll 2004) is used for front-end GA operations in this project because of its reliability and capability in modeling different GA operations. A comprehensive background on GAs can be found in Golberg (1989). The examples presented in this paper were executed using a simple GA with population size of 30, probability of crossover of 60%, and probability of mutation of 3.5%. Chromosomes of parents reproduce two child chromosomes in offspring generations with 4.0% probability of creep. New generations of chromosomes are produced until there is no increase in the fitness value of the best-fitted individual over the past 20 generations or the program stops at maximum number of generations equal to 300. It should be noted that intelligent GA operators (e.g., mutation, crossover) similar to the adaptive strategies used in this work have been introduced many years prior (Voss and Foley 1999, Schinler and Foley 2001,

Foley et al. 2002, Foley and Schinler 2003) and have been shown to be robust tools to solve very complicated optimization problems (Pezeshk et al. 2000, Foley and Schinler 2001, Alimoradi et al. 2004).

OPTIMIZATION FORMULATIONS

To study the influence of including the performance of nonstructural components in the design process, several optimization formulations were considered. In addition, the impact that elevating confidence levels for meeting nonstructural performance has on the weight (cost) of the structure was examined through these formulations. All of the cases studied have the same (high) level of confidence in meeting CP performance for the structural components based upon interstory global drift. In this manner, life safety of the structure is preserved.

Five fundamental, optimal design problem statements were formulated to evaluate the interaction between confidence in meeting structural component performance objectives and nonstructural component performance objectives. The fundamental optimization statements were formulated according to Equations 6–11 with the fitness evaluated as shown in Equation 12; the target damage state, the target confidence level, and the weight coefficients for each case are presented in Table 4.

Cases 1A through 1C facilitate evaluating the impact of increasing the confidence in meeting the slight damage state for NSD components on the structural weight (initial construction cost). Cases 2A through 2C are used to evaluate the impact of increasing confidence in meeting moderate damage to NSD components on the initial construction cost. Table 3 illustrates that drift limits for extensive and complete damage states for nonstructural components are larger than those for structural IO performance. This means that very high confidence levels need to be assured for IO performance when compared to those that would be considered to meet extensive and complete damage states. As a result, if all of these performance levels were considered in the same optimization problem, extensive and complete damage-state constraints would be inactive and design would be controlled solely by structural component performance. Therefore, nonstructural components were not considered in Cases 3A through 3C, and CP and IO performance levels were used instead. These cases allow the impact of elevating expectations in IO performance on the initial construction cost to be evaluated.

The economic impact of letting more damage to NSD components occur is evaluated using Cases 4A through 4D. Confidence levels in meeting NSD performance are maintained at 95% and the damage states considered for NSD components are elevated from slight to complete. As these damage states elevate, the resulting optimized design will give an indication of the premium that must be paid for reducing expected damage during the 50/50 events considered.

The impact of maximizing the confidence in meeting performance levels for NSA components required formulation of the optimization problem in an alternate manner. The median peak ground acceleration for the set of seven ground motions with 50% probability of exceedance in 50 years is 0.32 g. This would be the smallest peak floor acceleration (PFA) that the structure would experience, which results in low confidence

Table 4. Probabilistic optimal design problem statements

	Case	ds_{target} [a]	α_W	α_{CP}	q_{limit}^{IO}	α_{IO}	$q_{NSD,limit}^{ds}$	α_{NSD}	$q_{NSA,limit}^{ds}$	α_{NSA}	α_{SCWB}
	A						0.50				
1	B	Slight	0.3	0.3	I[b]	NA[c]	0.75	0.3	NA	NA	0.1
	C						0.95				
	A						0.50				
2	B	Moderate	0.3	0.3	I	NA	0.75	0.3	NA	NA	0.1
	C						0.95				
	A				0.50						
3	B	NA	0.3	0.3	0.75	0.3	NA	NA	NA	NA	0.1
	C				0.95						
4	A	Slight	0.3	0.3	NA	NA	0.95	0.3	NA	NA	0.1
	B	Moderate									
	C	Extensive									
	D	Complete									
	A				0.50				1.00		
5	B	Extensive	0.3	0.2	0.75	0.2	I	NA	1.00	0.2	0.1
	C				0.95				1.00		

[a] Target damage state for evaluating the performance of nonstructural components.
[b] *I* stands for inactive, meaning that such objective does not contribute to the fitness of the individual because the design is controlled by another performance.
[c] *NA*=Does not apply (e.g., an objective is not included in a given case, so the weight coefficient is zero).
Notes:
(i) All cases have a constant limit for confidence level at CP performance, $q_{limit}^{CP}=0.95$.
(ii) All cases have a constant limit for SCWB criteria, $(\Sigma M_{p,col}/\Sigma M_{p,beam})_{limit}=1.20$.
(iii) Case 3 does not include performance of nonstructural components in the design.
(iv) In Case 5, maximization of confidence level for performance of NSA components is intended so the $q_{NSA,limit}^{ds}=1.00$.

levels for the performance of the NSA components (i.e., $q_{NSA}^{slight}=45\%$, $q_{NSA}^{moderate}=85\%$, $q_{NSA}^{extensive}=98\%$, and $q_{NSA}^{complete}=99\%$). However, the design needs to be constrained to satisfy the required confidence in meeting CP and IO performance, which implies that higher floor accelerations need to be allowed in the formulation and, as a result, lower confidence levels in meeting PFA constraints must be expected. Therefore, Cases 5A through 5C attempt to find designs that minimize floor acceleration in the structure with inclusion of constraints for CP and IO performance. In this manner, the maximum possible confidence level for the performance of NSA components is calculated through an added objective of minimizing PFA during a set of events with 50% probability of exceedance in 50 years.

DISCUSSION OF RESULTS

The final designs for all five cases considered are summarized in Table 5. This table identifies the study case, and presents the weight of the structure, the column and beam cross-sections determined through application of automated design through the GA, and

Table 5. GA-generated designs for the different cases in study

Case	W kips	1st Floor			2nd Floor		
		Columns	Beam	M_{pc}/M_{pb}	Columns	Beam	M_{pc}/M_{pb}
1A	11.4	W33×152	W30×132	1.28	W30×108	W24×62	2.25
1B	17.5	W36×256	W36×160	1.67	W24×192	W21×132	1.68
1C	20.3	W40×331	W40×215	1.48	W30×132	W21×132	1.31
2A	9.0	W30×132	W24×104	1.51	W24×55	W10×68	1.58
2B	12.5	W36×160	W24×131	1.69	W21×57	W16×40	1.77
2C	17.3	W36×210	W21×122	2.71	W40×183	W24×176	1.53
3A	6.9	W36×135	W24×76	2.55	W14×43	W14×22	2.10
3B	7.3	W14×120	W21×73	1.23	W21×57	W16×40	1.77
3C	7.5	W21×132	W18×71	2.28	W24×55	W18×40	1.72
4A	20.3	W40×331	W40×215	1.48	W30×132	W21×132	1.31
4B	17.3	W36×210	W21×122	2.71	W40×183	W24×176	1.53
4C	7.3	W14×120	W16×89	1.20	W16×67	W16×36	2.06
4D	6.9	W14×145	W21×44	2.73	W10×60	W12×40	1.31
5A	9.9	W14×132	W14×90	1.49	W18×106	W16×67	1.74
5B	8.7	W12×190	W16×89	1.76	W10×60	W14×30	1.58
5C	7.8	W30×124	W16×67	3.09	W18×76	W21×44	1.71

the relative plastic moment capacity of girders and columns at every joint, to validate that the strong column-weak beam constraints are active. These columns of plastic moment capacity ratios also allow the impact of the problem formulation on column sizing to be evaluated.

Case 1 illustrates that there is a premium for elevating the confidence in meeting NSD components for the slight damage state. In other words, if one would like to have high confidence in the damage to NSD components being slight, then there appears to be a 78% increase in structural weight required to meet these expectations. Case 2 illustrates similar behavior when moderate damage confidence levels are elevated. Case 3 suggests that demanding increased confidence in meeting IO performance results in a moderate increase in weight. Case 4 confirms that when the damage state elevates (with consistent confidence in not exceeding), there is a corresponding reduction in the weight of the structural system. All this means is that if one allows more damage, one can pay less on the front end during construction. As expected, the first-floor columns (pinned bases) tend to drive the weight of the structural system chosen, as the first floor drift constraints will be very strict and difficult to satisfy without significant column moment of inertia.

Table 6 presents the weight of the structure, the median interstory drift for the two-level suites of ground motions considered, and the corresponding confidence levels for IO and CP performance of structural components as well as the performance of NSD components at each damage state. Case 1 illustrates that when confidence in not exceeding the slight NSD damage state elevates, confidence levels in not exceeding moderate,

Table 6. Performance information of structural and NSD components

Case	W kips	$ISDA$ 2POE50y	q^{CP} (%)	$ISDA$ 50POE50y	q^{IO} (%)	q^{NSD} (%)			
						Slight	Moderate	Extensive	Complete
1A	11.4	0.011705	**99**	0.003861	99	**53**	93	100	100
1B	17.5	0.006219	**99**	0.002862	99	**75**	98	100	100
1C	20.3	0.003088	**99**	0.001751	99	**95**	100	100	100
2A	9.0	0.019711	**99**	0.007967	99	8	**50**	99	100
2B	12.5	0.016068	**99**	0.005734	99	24	**75**	100	100
2C	17.3	0.011782	**99**	0.003533	99	60	**95**	100	100
3A	6.9	0.045437	**96**	0.013461	***56***	1	15	89	100
3B	7.3	0.046789	**95**	0.012130	***75***	1	20	93	100
3C	7.5	0.047224	**95**	0.009981	***95***	3	33	97	100
4A	20.3	0.003088	**99**	0.001751	99	**95**	100	100	100
4B	17.3	0.011782	**99**	0.003533	99	60	**95**	100	100
4C	7.3	0.045489	**96**	0.010977	88	2	26	**95**	100
4D	6.9	0.047668	**94**	0.021991	1	0	2	60	**95**
5A	9.9	0.047047	**95**	0.013818	***51***	1	14	88	99
5B	8.7	0.044560	**97**	0.012114	***75***	1	20	93	100
5C	7.8	0.046970	**95**	0.009948	***95***	3	33	97	100

extensive, and complete damage states remain very high. It appears that the slight damage states for NSD components can lead to improved IO performance as well. This was expected. Case 2 illustrates that while elevating levels of confidence in not exceeding the moderate damage state result in virtual assurance of not exceeding extensive and complete damage, there remain significant probabilities that slight damage will take place (i.e., 92% for Case 2A, 76% for Case 2B, and 40% for Case 2C). Case 3 illustrates that elevating levels of confidence in meeting IO performance does not guarantee acceptable confidence levels for not exceeding damage states for NSD components.

Case 4 illustrates rather interesting behavior. First of all, if slight and moderate NSD damage confidence levels are set high (i.e., 95%), then there will be a premium to be paid. There is a significant reduction in weight in the cases where extensive and complete damage-state confidence levels are high. It is also interesting to note that when confidence in meeting slight and moderate damage is high, there is 100% confidence in not exceeding the extensive and complete damage states for NSD components. However, if high confidence in not exceeding moderate damage is desired, there is a 40% chance that the slight damage state would be exceeded. Similarly, if 95% confidence in not exceeding extensive damage of NSD components is desired, there is a 75% probability that the moderate damage state will be exceeded. The results for Case 5 illustrate that elevating confidence in IO performance does not guarantee high levels of confidence in not exceeding NSD component damage states of moderate, extensive, and complete. However, as confidence in meeting IO performance exceeds 75%, confidence in not exceeding extensive and complete damage states for NSD components exceeds 90%.

Table 7. Performance information of structural and NSA components

Case	W kips	q^{CP} (%)	q^{IO} (%)	PFA (g) 50POE50y	q^{NSA} (%)			
					Slight	Moderate	Extensive	Complete
1A	11.4	**99**	99	0.856	4	28	71	96
1B	17.5	**99**	99	1.175	1	13	51	88
1C	20.3	**99**	99	0.804	5	31	75	97
2A	9.0	**99**	99	0.903	3	25	68	95
2B	12.5	**99**	99	0.926	3	24	67	94
2C	17.3	**99**	99	0.832	4	29	73	96
3A	6.9	**96**	**56**	1.153	1	14	53	89
3B	7.3	**95**	**75**	0.725	7	38	80	98
3C	7.5	**95**	**95**	0.758	6	35	78	97
4A	20.3	**99**	99	0.804	5	31	75	97
4B	17.3	**99**	99	0.832	4	29	73	96
4C	7.3	**96**	88	0.744	6	36	79	97
4D	6.9	**94**	1	1.141	1	14	53	89
5A	9.9	**95**	**51**	0.685	8	41	***82***	98
5B	8.7	**97**	**75**	0.767	6	34	*77*	97
5C	7.8	**95**	**95**	0.752	6	35	***78***	97

Table 7 summarizes the weight of the structure, the confidence levels for IO and CP performance of structural components, the median PFA under a set of seven ground motions with 50% probability of exceedance in 50 years, and the corresponding confidence levels for not exceeding each damage state for NSA components. As can be seen in the table, the final designs satisfy the constraints that were formulated in order to achieve the confidence required in the performance of every case in study. The results in the table indicate that constraints on CP and IO performance have relatively little bearing on confidence in not exceeding NSA component damage states.

Figure 4 illustrates the variation of the structural weight, the confidence level for the performance of structural components, as well as the discrete probabilities of damage for each damage state for NSD components. Figure 5 illustrates the variation of the structure weight and the discrete probabilities of damage for each damage state for NSA components. The confidence levels in meeting any damage state, which are shown in Tables 6 and 7, can be inferred from the probabilities of damage in Figures 4 and 5 as follows:

$$q^{slight} = 1 - (P[Slight] + P[Moderate] + P[Extensive] + P[Complete])$$

$$q^{moderate} = 1 - (P[Moderate] + P[Extensive] + P[Complete])$$

$$q^{extensive} = 1 - (P[Extensive] + P[Complete])$$

$$q^{complete} = 1 - (P[Complete]). \tag{16}$$

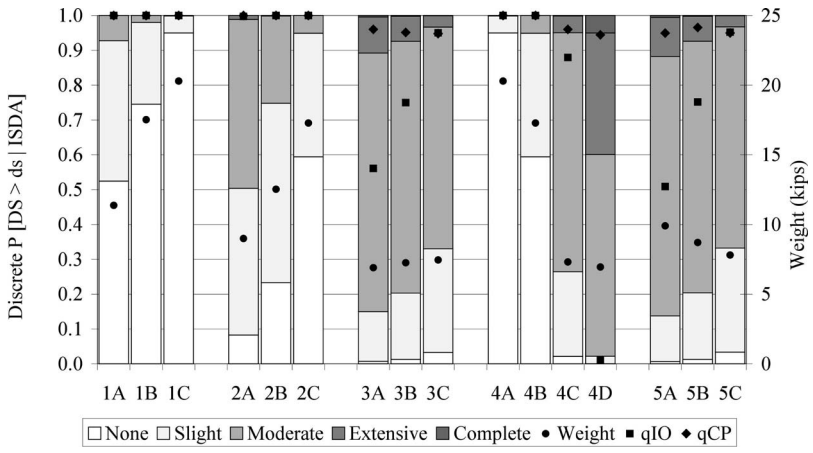

Figure 4. Performance of structural and NSD components: Cases 1 through 5.

The discrete probabilities of damage for NSD components corresponding to Case 4D as illustrated in Figure 4 are 2%, 58%, 35%, and 5% for slight, moderate, extensive, and complete damage states, respectively. Therefore, for Case 4D, the confidence level in meeting each damage state can be inferred from Figure 4 and read from Table 6 as $q_{NSD}^{Slight}=0\%$, $q_{NSD}^{Moderate}=2\%$, $q_{NSD}^{Extensive}=60\%$, and $q_{NSD}^{Complete}=95\%$.

As expected, Figure 4 and Table 6 illustrate that the weight of the structure increases as the confidence level in meeting performance increases. This is seen by considering the weight moving from Case 1A to 1C, Case 2A to 2C, and Case 3A to 3C. For the NSD components, the high variability of each damage state ($\beta_{ds}=0.5$) results in small

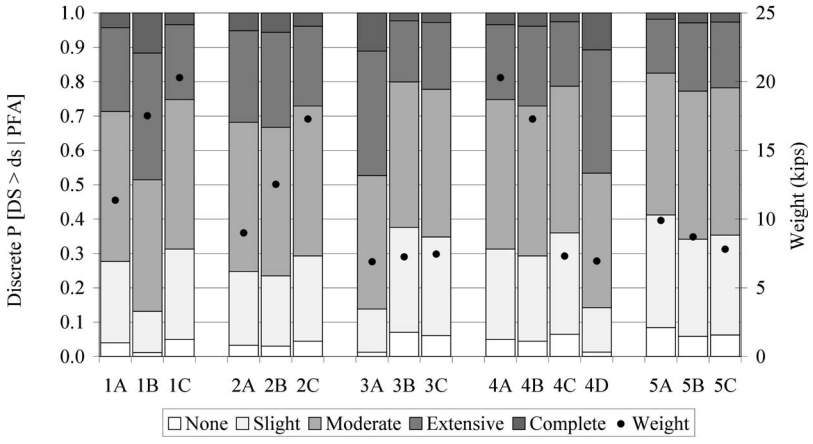

Figure 5. Performance of NSA components: Cases 1 through 5.

increases in the confidence level leading to a very large reduction in the drift limit and, therefore, a large increase in the stiffness of the structure. There is an average weight increase of 45% as the confidence in meeting NSD performance increases from $q_{NSD}=50\%$ to $q_{NSD}=95\%$. On the other hand, increasing the confidence level for IO performance of structural elements from $q^{IO}=50\%$ to $q^{IO}=95\%$ required just a slight increment of the weight of the structure for Case 3A to 3C. These results suggest that if the structural-engineering community can understand damage to nonstructural drift-sensitive components more thoroughly (i.e., reduce the variability in damage state thresholds), it can have significant economic impact on designs that will result through application of the performance-based design methodologies currently under development. Furthermore, the HAZUS NSD fragility curves have a much greater impact on initial construction cost than the IO structural performance fragility curves.

Through examination of the floor accelerations for the cases where the confidence level was fixed at 95% for each NSD damage state (Case 4A through 4D), the ability for target NSD performance objectives indirectly resulting in good NSA component performance can be evaluated. The results shown in Tables 6 and 7 and Figures 4 and 5 illustrate that the NSA components will have a high probability that slight or moderate damage will occur even though high confidence in meeting NSD performance is expected. If one looks at Case 4A and 4B in Tables 6 and 7 and Figures 4 and 5, it can be seen that even though there is 95% confidence in meeting slight and moderate performance levels for NSD components, there is only 5% and 29% confidence in meeting NSA component performance at these same states of slight and moderate, respectively. The disparities in NSD and NSA performance tend to reduce when extensive and complete damage states are considered.

Figure 4 and Table 6 also illustrate that when the extent of damage to NSD components elevates (Case 4A through 4D), the confidence level in meeting CP and IO performance for structural components decreases. This means that for slight (point *a*) and moderate (point *b*) damage states, the design can be controlled by the performance of nonstructural drift-sensitive components. However, for extensive (point *d*) and complete (point *e*) damage states, the design would be controlled by the IO (point *c*) performance of the structural components. This behavior can be seen clearly in Figure 6, where for any given confidence level the drift limit to meet slight damage, d_{NSD}^{slight}, is less than $d_{NSD}^{moderate} < d^{IO} < d_{NSD}^{extensive} < d_{NSD}^{complete} < d^{CP}$ (i.e., for $q=75\%$, $a<b<c<d<e$). In other words, when the design requires maximizing the confidence in the NSD component performance for slight or moderate damage, the constraint to assure IO performance would be inactive. Moreover, when the design requires maximizing the confidence in the performance of NSD components for extensive or complete damage, the constraint to assure IO performance would be active and the one for NSD components would be inactive. This demonstrates that there can be a reduction in the number of performance objectives for immediate occupancy–type performance, and also that slight and moderate NSD component performance objectives along with IO structural performance objectives are sufficient to capture design needs.

As explained earlier, since the median peak ground acceleration for the set of seven ground motions with less than 50% probability of exceedance in 50 years is 0.32 g, no

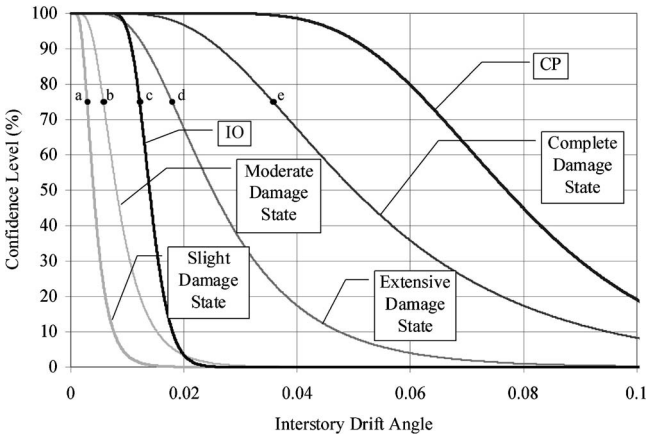

Figure 6. Confidence level curves for structural and NSD components.

design would provide a high confidence level in meeting CP performance and slight or moderate damage for nonstructural acceleration-sensitive components at the same time. However, by analyzing the results obtained for Case 5 (Tables 5 and 6, Figures 4 and 5), a design can be achieved that satisfies the constraints for the IO and CP performance and provides high confidence levels for the performance of NSD and NSA components meeting the extensive damage state. Figures 4 and 5 indicate that with confidence in meeting CP and IO structural performance objectives very high ($q^{CP}=50\%$ and $q^{IO}=95\%$), there is very high confidence in meeting the extensive damage state for NSD components ($d_{NSD}^{extensive}=96\%$) and high confidence in meeting NSA component performance ($d_{NSA}^{extensive}=78\%$).

PARETO FRONT

The previous discussion illustrates that confidence in meeting confidence levels for NSD and NSA performance is a conflicting objective. As a result, a true two-objective optimization problem was formulated and Pareto fronts were defined using the dynamic weighted aggregation method. The two objectives to be minimized are the ISDA and the PFA. This optimization problem is solved using a GA with the fitness of individual j at generation k during the evolution, evaluated as:

$$F_{jk}=w_1(t)\cdot\left(\frac{ISDA_{max}-ISDA_{jk}}{ISDA_{max}}\right)+w_2(t)\cdot\left(\frac{PFA_{max}-PFA_{jk}}{PFA_{max}}\right) \tag{17}$$

where $ISDA_{max}$ and PFA_{max} are the maximum expected values for the topology and ground motion records used in this study; and $ISDA_{jk}$ and PFA_{jk} are the values corresponding to design j in generation k. $w_1(t)$ and $w_2(t)$ are weights that are changed gradually according to Equation 18 in order to force the GA to keep moving on the Pareto front:

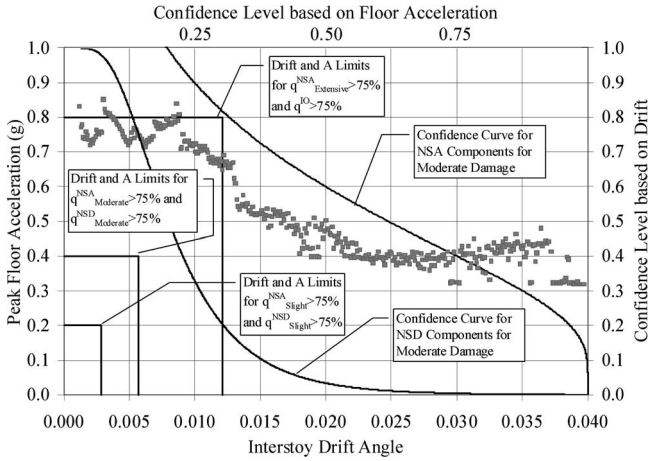

Figure 7. Pareto front for floor acceleration and interstory drift for 50POE50.

$$w_1(t) = |\sin(2\pi t/F)|$$

$$w_2(t) = 1.0 - w_1(t) \tag{18}$$

where t is the number of runs of the GA, and f is a constant to adjust the change frequency.

For every combination of weights, the GA will find a stable minimum with the same stopping criteria explained before; next, the weights are changed gradually until all the solutions on the front are obtained. Figure 7 shows a Pareto front for the two design objectives. The interstory drift and floor acceleration limits corresponding to a 75% confidence in meeting slight and moderate damage for NSD components and IO performance for structural components are also indicated.

It can be seen that if the design constraints require $q_{NSD}^{slight} \geqslant 75\%$ and $q_{NSA}^{slight} \geqslant 75\%$ or $q_{NSD}^{moderate} \geqslant 75\%$ and $q_{NSA}^{moderate} \geqslant 75\%$ there would not be a solution possible for the structural topology and ground motions used in this study. However, there are some designs that have $q^{IO} \geqslant 75\%$ and $q_{NSA}^{extensive} \geqslant 75\%$. In these cases, alternate structural systems that include supplemental damping and/or base isolation technologies may be required. This is the natural response that structural engineers would utilize in this situation, but it is very encouraging to realize that the automated design algorithm presented would facilitate this type of decision making automatically. Furthermore, with the Pareto fronts used for decision-making purposes, the structural engineer would have a graphical way to explain these decisions to clients.

CONCLUDING REMARKS

The formulation of a performance-based optimization problem that included target confidence levels in meeting structural and nonstructural component performance objec-

tives was discussed. Several optimization problems designed to explore the synergy between initial construction cost (simulated through weight) and performance were outlined. These optimization problems were solved using a genetic algorithm, and the GA-based designs were discussed in great detail. A multiple-objective optimization problem was also formulated to include competing objectives of confidence in meeting performance objectives for nonstructural drift-sensitive and nonstructural acceleration-sensitive components. This optimization problem was also solved using a GA-based methodology.

The algorithm used in this study was capable of presenting designs with minimum weight that satisfy predefined ranges of preferred seismic performance. The weight of the structure seemed to be very sensitive to an increment in the target confidence level for the performance of nonstructural components. Even though it was possible to achieve high confidence levels for the performance of both structural and NSD components, NSA components had high probabilities of damage in most cases. Floor accelerations, interstory drift, and weight of the structure are three competing objective functions. While high confidence levels for the performance of both structural and NSD components require a stiffer structure, high confidence levels for the performance of NSA components require a softer structure. The designs obtained for Case 5 have the best performance obtained for the structure and ground motions in study. Those designs have confidence levels of 95% for IO and CP performance of structural components, and 95% and 78% that NSD and NSA components, respectively, will not have extensive damage.

As stated previously, the results obtained for the two-story frame and ground motions considered suggest that if the structural-engineering community can understand damage to nonstructural drift-sensitive components more thoroughly (i.e., reduce the variability in damage state thresholds), it can have significant economic impact on designs that will result through application of the performance-based design methodologies currently under development. Furthermore, the NSD fragility curves have a much greater impact on initial construction cost than the IO structural performance fragility curves.

Optimization problems that include objectives of confidence in meeting NSD performance and confidence in meeting NSA performance appear to present unique challenges for the structural engineer. In these cases, alternate structural systems that include supplemental damping and/or base isolation technologies may be required. As stated, this is the natural response that structural engineers would utilize in this situation, but it is very encouraging to realize that the automated design algorithm presented would facilitate this type of decision making automatically. Furthermore, with the Pareto fronts used for decision-making purposes, the structural engineer would have a graphical way to explain these decisions to clients.

The design examples considered demonstrate that there may be opportunity to reduce the number of performance objectives used in a design effort. For example, when a design requires maximizing the confidence in meeting NSD component performance for the damage states of slight and moderate, constraints related to confidence in meeting IO

structural performance are not necessary. These were shown to be inactive during the GA runs. In a similar manner, if IO structural performance objectives are implemented, then there is no need to include constraints on maximizing the confidence in seeing damage states for NSD components less than extensive or complete.

The present effort is not without minor shortcomings. A limited number of ground motions and a relatively small structural system were considered. Also, the HAZUS fragility curves are approximate. The algorithms described in this study are scalable to any structural system provided the structural engineer can describe fragility functions for structural and nonstructural component performance. As the structural-engineering profession develops more accurate fragility curves for structural systems, structural components, NSD components, and NSA components, the algorithms described are ready-made to incorporate these relationships as they evolve. Furthermore, as long as the structural engineer can define ground motions with the needed characteristics to describe the seismic hazard at a building's location, and provided the analytical engine to analyze the structural system exists, the algorithms developed can easily be used as the basis for algorithms that involve more complex analysis approaches and as many ground motions as desired.

REFERENCES

AISC, 2005. *Load and Resistance Factor Specifications for the Design of Steel Buildings*, American Institute of Steel Construction, Chicago, Ill.

Algan, B., 1982. Drift and Damage Considerations in Earthquake Resistant Design of Reinforced Concrete Buildings, Ph.D. Dissertation, University of Illinois, Urbana-Champaign.

Alimoradi, A., 2004. Probabilistic Performance-Based Seismic Design Automation of Nonlinear Steel Structures Using Genetic Algorithms, Ph.D. Thesis, University of Memphis, Tenn.

Alimoradi, A., and Ahmadi, G., 2002. Sensitivity analysis of a GA-based active/hybrid control system under near-source strong ground motion, *7th U.S. National Conference on Earthquake Engineering (7NCEE)*, Boston, Mass.

Alimoradi, A., Pezeshk, S., and Foley, C. M., 2004. *Automated Performance-Based Design of Steel Frames*, ASCE Structures Congress and Exposition, Nashville, Tenn. [CD-ROM].

———, 2007. Probabilistic performance-based optimal design of steel moment-resisting frames: part II—applications, *J. Struct. Eng.* **133**, 767–776.

ATC, 1996. *Seismic Evaluation and Retrofit of Existing Concrete Buildings: Volumes 1 and 2*, Applied Technology Council, Redwood City, Calif.

Carroll, D. L., 2004. *FORTRAN Genetic Algorithm Driver*, CU Aerospace, Champaign, Ill. (available at: http://cuaerospace.com/carroll/ga.html).

Comerio, M. C., Stallmeyer, J. C., Holmes, W. T., Morris, P., and Lau, S., 2002. *Nonstructural Loss Estimation: The UC Berkeley Case Study, PEER Report 2001/01*, Pacific Earthquake Engineering Research Center, Berkeley, Calif.

FEMA, 2000. *FEMA-350: Recommended Seismic Design Criteria for New Steel Moment-Frame Buildings*, Federal Emergency Management Agency, Washington, D.C.

———, 2003. *Multi-Hazard Loss Estimation Methodology Earthquake Model: HAZUS-MH MR1*, Department of Homeland Security Emergency Preparedness Response Directorate, Washington, D.C.

Filiatrault, A., Christopoulos, C., and Stearns, C., 2002. *Guidelines, Specifications, and Seismic Performance Characterization of Nonstructural Building Components and Equipment, PEER Report 2002/05*, Pacific Earthquake Engineering Research Center, Berkeley, Calif.

Foley, C. M., 2002. Optimized performance-based design for buildings, in *Recent Advances in Optimal Structural Design*, edited by S. A. Burns, American Society of Civil Engineers, Reston, VA, 169–240.

Foley, C. M., Alimoradi, A., and Pezeshk, S., 2007. Probabilistic performance-based optimal design of steel moment-resisting frames: part 1, *J. Struct. Eng.* **133**, 757–766.

Foley, C. M., and Schinler, D., 2001. Optimized design of steel frames using distributed plasticity, in *2001 Structures Congress*, edited by P. Chang, American Society of Civil Engineers, Washington, D.C. [CD-ROM].

———, 2003. Automated design of steel frames using advanced analysis and object-oriented evolutionary computation, *J. Struct. Eng.* **129**, 648–660.

Foley, C. M., Schinler, D., and Voss, M. S., 2002. *Optimized Design of Fully and Partially Restrained Steel Frames Using Advanced Analysis and Object-Oriented Evolutionary Computation*, Technical report submitted to the National Science Foundation, Award Number CMS-9813216.

Fragiadakis, M., Lagaros, N. D., and Papadrakakis, M., 2006. Performance-based multiobjective optimum design of steel structures considering life-cycle cost, *Struct. Multidiscip. Optim.* **32**, 1–11.

Golberg, D. E., 1989. *Genetic Algorithms in Search, Optimization, and Machine Learning*, Addison-Wesley, Boston, Mass.

Holmes, W. T., and Comerio, M. C., 2003. *Implementation Manual for the Seismic Protection of Laboratory Contents: Format and Case Studies, PEER Report 2003/12*, Pacific Earthquake Engineering Center, Berkeley, Calif.

Jalayer, F., and Cornell, C. A., 2003. *A Technical Framework for Probability-Based Demand and Capacity Factor (DCFD) Seismic Formats, PEER Report 2003/08*, Pacific Earthquake Engineering Research Center, Berkeley, Calif.

Kim, Y., and Ghaboussi, J., 1999. A new method of reduced-order feedback control using genetic algorithms, *Earthquake Eng. Struct. Dyn.* **28**, 235–254.

Liu, M., 2004. Development of Multiobjective Optimization Procedures for Seismic Design of Steel Moment Frame Structures, Ph.D. Dissertation, Department of Civil and Environmental Engineering, University of Illinois, Urbana-Champaign.

Liu, M., Burns, S. A., and Wen, Y. K., 2003. Optimal seismic design of steel frame buildings based on life-cycle cost considerations, *Earthquake Eng. Struct. Dyn.* **32**, 1313–1332.

———, 2004. Life cycle cost oriented seismic design optimization of steel moment frame structures with risk taking preference, *Eng. Struct.* **26**, 1407–1421.

———, 2005. Multiobjective optimization for performance-based seismic design of steel moment frame structures, *Earthquake Eng. Struct. Dyn.* **34**, 289–306.

———, 2006. Genetic algorithm based construction-conscious minimum weight design of seismic steel moment-resisting frames, *J. Struct. Eng.* **132**, 50–58.

Naeim, F., Alimoradi, A., and Pezeshk, S., 2004. Selection and scaling of ground motion time histories for structural design using genetic algorithms, *Earthquake Spectra* **20**, 413–426.

Pezeshk, S., Camp, C. V., and Chen, D., 1997. Optimal design of 2D frames using a genetic

algorithm, *Optimal Performance of Civil Infrastructure Systems at Structures Congress XV, Portland, OR*, 155–168.

———, 2000. Design of framed structures using genetic optimization, *J. Struct. Eng.* **126**, 382–388.

Powell, G. H., 1993. *DRAIN-2DX Element Description and User Guide for Element Type01, Type02, Type04, Type06, Type09, and Type15: Version 1.10, UCB/SEMM-93/18*, University of California, Berkeley.

Prakash, V., Powell, G. H., and Campbell, S., 1993. *DRAIN-2DX Base Program Description and User Guide, Version 1.10, Report No. UCB/SEMM-93/17–18*, University of California, Berkeley.

Schinler, D., and Foley, C. M., 2001. An object-oriented evolutionary algorithm for advanced analysis-based design, *Proceedings of the Genetic and Evolutionary Computation Conference (GECCO)*, edited by S. A. Burns, Morgan Kaufmann, San Francisco, Calif., 73–78.

Somerville, P., Smith, N. F., Punyamurthula, S., and Sun, J., 1997. *Development of Ground Motion Time Histories for Phase 2 of the FEMA/SAC Steel Project, Report No. SAC/BD-97-04*, SAC Joint Venture, Sacramento, Calif.

Taghavi, S., and Miranda, E., 2003. *Response Assessment of Nonstructural Building Elements, PEER Report 2003/05*, Pacific Earthquake Engineering Research Center, Berkeley, Calif.

Voss, M. S., and Foley, C. M., 1999. Evolutionary algorithm for structural optimization, *Proceedings of the Genetic and Evolutionary Computation Conference (GECCO)*, edited by W. Banzhaf, J. Daida, A. E. Eiben, M. H. Garzon, V. Honavar, M. Jakiela, and R. E. Smith, Morgan Kaufman, San Francisco, Calif., 678–685.

(Received 31 July 2006; accepted 12 April 2007)